

## Electronic Supplementary Information

### Detecting Single-Point Isomeric Differences in Polymer Chains by MOF Column Chromatography

Nobuhiko Hosono,\* Yu Kono, Nagi Mizutani, Daichi Koga, Takashi Uemura\*

#### 1. General Instrumentations

<sup>1</sup>H nuclear magnetic resonance (NMR) spectra were recorded using a Bruker Avance III HD spectrometer equipped with a PABBO probe operating at 500 MHz. Powder X-ray diffraction (PXRD) data were recorded on a Rigaku model SmartLab X-ray diffractometer using Cu K $\alpha$  radiation. Analytical size-exclusion chromatography (SEC) measurements were performed using two polystyrene gel columns in series (Shodex KF-806M) at 40 °C on a SHIMADZU model LC-2050 system equipped with a refractive index (RI) detector. The mobile phase was tetrahydrofuran (THF) at a flow rate of 1.0 mL min<sup>-1</sup>. Scanning electron microscopy (SEM) measurements were performed using a Hitachi model SU-5000 at an accelerating voltage of 15 kV. Samples were deposited on a conducting carbon tape attached on a SEM sample holder, then coated with osmium. Purification by recycling preparative SEC was conducted using LaboACE LC5060 system connected with two columns in series (JAIGEL-2.5HR and JAIGEL-2HR). The mobile phase was chloroform at a flow rate of 10.0 mL min<sup>-1</sup>.

#### 2. Materials

All reagents and chemicals used in this study were obtained from, FUJIFILM Wako Pure Chemicals, and Tokyo Chemical Industry (TCI), unless otherwise noted. Deuterated solvents for NMR spectroscopy were purchased from KANTO CHEMICAL CO., INC. Polyethylene glycol monomethyl ether 1000 (PEG1k,  $M_n = 1000$ ) was purchased from TCI and used without further purification.

**Synthesis of 1.** [Zn<sub>2</sub>(1,4-naphthalenedicarboxylate)<sub>2</sub>triethylenediamine]<sub>n</sub> (**1**) was synthesized according to the previously reported procedure with a slight modification.<sup>S1,S2</sup> The solvothermal synthesis was performed with stirring the reaction mixture to have a better control of particle size of **1**. *N,N*-dimethylformamide (DMF) (250 mL) solution of Zn(NO<sub>3</sub>)<sub>2</sub>·4H<sub>2</sub>O (5.2 g, 20 mmol), 1,4-naphthalenedicarboxylic acid (4.3 g, 20 mmol) and triethylenediamine (1.1 g, 10 mmol) was stirred vigorously at 120 °C for 64 h. The reaction mixture was then cooled to room temperature and the product was collected by suction filtration. The white powder thus obtained was washed with DMF (ca. 50 mL × 3) then methanol (ca. 50 mL × 1). The powder was collected by centrifugation, and then dried under vacuum for 16 h, affording **1** in a powder form (5.8 g) (Fig. S1 and S2).

**Preparation of *o*-PEG.** Under a nitrogen atmosphere, excess NaH (100 mg) and **PEG1k** (2.0 mmol, 2.0 g) were added to 25 mL of anhydrous acetonitrile. Subsequently, an anhydrous acetonitrile solution (10 mL) of  $\alpha,\alpha'$ -dibromo-*o*-xylene (1.00 mmol, 264 mg) was added to the mixture, then the mixture was stirred at 40 °C for 24 h. After cooling to room temperature, the solid residue was removed by filtration. The crude product was obtained by extraction with chloroform. The product was subjected to recycling preparative SEC to remove unreacted materials, affording ***o*-PEG**. The final product was analyzed by analytical SEC, which showed a monomodal peak and no signals corresponding to the starting material or byproducts (Fig. S3, Table S1).

$^1\text{H NMR}$  (500 MHz,  $\text{DMSO-}d_6$ ):  $\delta$  (ppm) 7.36-7.38 (m, Ar, 2H), 7.27-7.28 (m, Ar, 2H), 4.54 (s, 4H), 3.43- 3.59 (br, 160H), 3.24 (s, 6H).

**Preparation of *m*-PEG.** Under a nitrogen atmosphere, excess NaH (240 mg) and **PEG1k** (2.0 mmol, 2.0 g) were added to 25 mL of anhydrous acetonitrile. Subsequently, an anhydrous acetonitrile solution (10 mL) of  $\alpha,\alpha'$ -dibromo-*m*-xylene (0.500 mmol, 132 mg) was added to the mixture, then the mixture was stirred at 50 °C for 24 h. After cooling to room temperature, the solid residue was removed by filtration. The crude product was obtained by extraction with chloroform. The product was subjected to recycling preparative SEC to remove unreacted materials, affording ***m*-PEG**. The final product was analyzed by analytical SEC, which showed a monomodal peak and no signals corresponding to the starting material or byproducts (Fig. S3, Table S1).

$^1\text{H NMR}$  (500 MHz,  $\text{CDCl}_3$ ):  $\delta$  (ppm) 7.29-7.20 (m, Ar), 4.48 (s, 4H), 3.44–3.60 (br, 174H). The aromatic peaks overlapped with the peak of residual protons of  $\text{CDCl}_3$ .

**Preparation of *p*-PEG.** Under a nitrogen atmosphere, excess NaH (200 mg) and **PEG1k** (2 mmol, 2.0 g) were added to 25 mL of anhydrous acetonitrile. Subsequently, an anhydrous acetonitrile solution (10 mL) of  $\alpha,\alpha'$ -dibromo-*p*-xylene (1.00 mmol, 264 mg) was added to the mixture, then the mixture was stirred at 50 °C for 24 h. After cooling to room temperature, the solid residue was removed by filtration. The crude product was obtained by extraction with chloroform. The product was subjected to recycling preparative SEC to remove unreacted materials, affording ***p*-PEG**. The final product was analyzed by analytical SEC, which showed a monomodal peak and no signals corresponding to the starting material or byproducts (Fig. S3, Table S1).

$^1\text{H NMR}$  (500 MHz,  $\text{CDCl}_3$ ):  $\delta$  (ppm) 7.31 (s, 4H), 4.55 (s, 4H), 3.60–3.68 (br, 184H), 3.38 (s, 6H).

**Preparation of *n*-PEG.** Under a nitrogen atmosphere, powdered KOH (5.00 mmol, 280 mg) was dispersed in 5 mL of tetrahydrofuran (THF)/heptane (75/25, v/v) and heated to 40 °C. Subsequently, an anhydrous THF solution of **PEG1k** (1.00 mmol, 1.00 g) and *p*-toluenesulfonyl chloride (95.0 mg, 0.500 mmol) was added dropwise. The mixture was then stirred for 24 h at 40 °C. The precipitates were removed by filtration, and the solution was evaporated to dryness under a reduced pressure.

Subsequently, 50 mL of water was added, and the solution was neutralized with an aqueous solution of  $\text{NH}_4\text{Cl}$ . The product was recovered by extraction with chloroform ( $10 \text{ mL} \times 3$ ), then subjected to recycling preparative SEC to remove unreacted materials, affording ***n*-PEG**. The final product was analyzed by analytical SEC, which showed a monomodal peak and no signals corresponding to the starting material or byproducts (Fig. S3, Table S1).

$^1\text{H}$  NMR (500 MHz,  $\text{CDCl}_3$ ):  $\delta$  (ppm) 3.58–3.74 (br, 184H), 3.38 (s, 6H).

### 3. HPLC Analysis on the MOF Column

A **1**-packed column was prepared according to the previously reported procedure.<sup>(S2)</sup> A stainless-steel column (I.D. = 4 mm, L. = 150 mm; GL Sciences model 6010-11043) was packed with powdery crystals of **1** (0.75 g, particle diameter: 3-10  $\mu\text{m}$ , Fig. S2) by a tapping method. The **1**-packed column was connected to a Shimadzu HPLC Prominence system equipped with an evaporative light scattering detector (ELSD) (Shimadzu ELSD-LTII). GPC-grade DMF (FUJIFILM Wako Pure Chemicals) was used as a mobile phase. The PEG samples were dissolved in DMF ( $1 \text{ mg mL}^{-1}$ ) and injected into the column (injection volume: 30  $\mu\text{L}$ ). The chromatograms were recorded at given temperatures and flow rates of the mobile phase. The retention factor,  $k = (t_{\text{R}} - t_0)/t_0$ , where  $t_{\text{R}}$  is an observed retention time and  $t_0$  is a column hold-up time, was calculated for each PEG sample. The corrected retention time,  $t_{\text{c}}$ , is defined as  $t_{\text{c}} = t_{\text{R}} - t_0$ .  $t_0$  was determined using the elution peak of 1,3,5-triphenylbenzene (TPB) which is larger than the pore size of **1**.<sup>S2,S3</sup>

Three **1**-packed columns were prepared using the method described above, and the retention times of the PEG samples were measured on each column. The observed  $k$  values under the respective conditions are shown in Fig. 3a, presented as mean  $\pm$  standard deviation ( $N = 3$ ).

The number of theoretical plates ( $N$ ) and separation resolution ( $R_{\text{s}}$ ) for ***o*-**, ***m*-**, and ***p*-PEG** relative to ***n*-PEG** on the **1** column were calculated using the half-width method, and the results are summarized in Table S2. The relatively low  $N$  values observed for the **1** column can be attributed to the irregular sizes and shapes of the MOF particles and the slow adsorption kinetics of the PEGs, which contribute to the broadening of the elution peaks.<sup>S4</sup>

### 4. Adsorption Kinetics Measurement

Adsorption kinetics were measured using a batch adsorption method with **1** in powder form and ethanol solutions of the respective PEGs. Ethanol was used as the solvent instead of DMF, as PEG adsorption in DMF is minimal and difficult to quantify with sufficient accuracy in this system.<sup>S4</sup> Ethanol, on the other hand, results in significant adsorption within a reasonable timeframe, allowing for a more accurate and reliable kinetic study.

An ethanol solution of PEG was prepared in a glass vial, which was placed in an oil bath thermostated at 40  $^{\circ}\text{C}$ . For ***o*-PEG** and ***p*-PEG**, 60 mg of PEG and 50.0 g of ethanol were used. For ***m*-PEG**, 30 mg of PEG and 25.0 g of ethanol were used. Activated **1** was gently added to the PEG solution (190 mg each for ***o*-PEG** and ***p*-PEG**, and 95.0 mg for ***m*-PEG**) and the solution was stirred vigorously.

A small aliquot of the supernatant was removed from the vial at a given time interval after the addition of **1**. The adsorbed amount of PEG normalized with the MOF unit weight was determined by  $^1\text{H}$  NMR analysis.

The adsorption amount of PEG into the MOF was determined by quantification of the PEG concentration of the supernatant solution phase according to the previously reported procedure.<sup>S3,S4</sup> The amount of PEG adsorbed in a unit weight (1 g) of MOF ( $m_{ad}$ ) is described as,

$$m_{ad} = \frac{(c_0 - c_t)m_1}{m_2}$$

where  $c_0$  is the initial concentration of the PEG solution used,  $c_t$  is the PEG concentration of the supernatant solution after the given adsorption time,  $m_1$  is the amount of the PEG solution, and  $m_2$  is the amount of MOF added in the solution.  $c_t$  was quantified by using  $^1\text{H}$  NMR as follows. A negligibly small aliquot of the supernatant was taken from the parent suspension into a glass vial. After thorough removal of the solvent in the vial by evaporation, the remaining solid residue (PEG) was dissolved in deuterated chloroform with an external reference (toluene). The concentration of the reference compound was fixed at 50  $\mu\text{L}$  per 30 mL of deuterated chloroform, thus allowing quantification of PEG amount in the residue of the supernatant solution by using  $^1\text{H}$  NMR analysis.

Based on the integration areas of proton signals for PEG (methylene protons) and the reference compound,  $c_t$  was calculated by the following equation,

$$c_t = \frac{1}{m_3} \left( \frac{m_4 \times \frac{Rc^*}{R_0}}{1 - \frac{Rc^*}{R_0}} \right),$$

where  $c^*$  is the concentration of the reference compound,  $R_0$  is the peak area ratio between PEG and the reference compound of the initial solution (before MOF addition),  $R$  is the peak area ratio between PEG and the reference compound after given adsorption time,  $m_3$  is the weight of the supernatant sample taken from the parent suspension, and  $m_4$  is the weight of the deuterated chloroform added to the vial in order to perform  $^1\text{H}$  NMR analysis.

## 5. Molecular Dynamics Simulation

All the molecular dynamics (MD) simulations were performed using the LAMMPS program.<sup>S5</sup> The MD snapshots were generated using OVITO software.<sup>S6</sup> We used the particle mesh Ewald (PME) procedure to handle long-range electrostatic interactions under periodic boundary conditions. The cut-off parameter was set to 10 Å. The force field parameters were determined by the same method as in our previous study.<sup>S7</sup> The integration time step was 2 fs, and the SHAKE method was applied to constrain the bonds involving hydrogen atoms.

The shortened versions of PEGs (20 mer), HO-(CH<sub>2</sub>-CH<sub>2</sub>-O)<sub>10</sub>-CH<sub>2</sub>-C<sub>6</sub>H<sub>4</sub>-CH<sub>2</sub>-(O-CH<sub>2</sub>-CH<sub>2</sub>)<sub>10</sub>-OH, with *ortho*-, *meta*-, and *para*-substituted xylene moiety at the center were generated and used as the models of *o*-PEG, *m*-PEG, and *p*-PEG. The superlattice of **1** was built by aligning 3 × 3 × 12 unit cells in the *a*-, *b*-, and *c*-axis directions, respectively. Each unit cell has dimensions of 10.921

$\times 10.921 \times 9.611 \text{ \AA}^3$ . The {001} surface of **1**, where the pore entrance opens for PEG insertion, consists of the Zn paddlewheel clusters remaining the exposed Zn coordination sites open.

Initially, the framework of **1** and the 15 molecules of the guest PEG were independently equilibrated by an MD run for 5 ns at 393 K in an  $NVT$  condition. Then, the PEG molecules were placed on one side of the {001} surface of the **1** framework. Finally, an MD run for the PEG infiltration was executed for 100 ns at 393 K in an  $NVT$  condition. The MD simulation was performed for *o*-PEG, *m*-PEG, and *p*-PEG and repeated 5 times for each PEG. The center of mass (COM) of all PEG molecules in the simulation cell was recorded. The representative COMs of the PEG molecules for a typical MD run are plotted as a function of infiltration time in Fig. S5. The COM data of the 5 runs for each PEG was summarized in Fig. 4c with a standard deviation band.

## 6. Supporting Table

**Table S1.** SEC data of the model PEGs used in this study.<sup>a</sup>

Code	$M_n$ (g/mol)	$M_w$ (g/mol)	$\bar{D}$
<i>o</i> -PEG	2180	2310	1.06
<i>m</i> -PEG	2060	2230	1.08
<i>p</i> -PEG	2010	2190	1.08
<i>n</i> -PEG	2010	2090	1.04

<sup>a</sup>Standard PEGs were used for molecular weight calibration.

**Table S2.** Retention time ( $t_R$ )<sup>a</sup> and the number of theoretical plate ( $N$ )<sup>b</sup> of the **1** column, calculated for *o*-, *m*-, *p*-, and *n*-PEG, and separation resolution ( $R_s$ )<sup>a</sup> of *o*-, *m*-, and *p*-PEG against *n*-PEG,

	<i>o</i> -PEG	<i>m</i> -PEG	<i>p</i> -PEG	<i>n</i> -PEG
$t_R$	1.63 min	3.24 min	3.86 min	4.10 min
$N$	36.3	16.4	22.7	34.7
$R_s$	1.28	0.29	0.08	–

<sup>a</sup>Injection volume: 30  $\mu\text{L}$ ; Column temperature: 80  $^\circ\text{C}$ ; Flow rate: 1.0 mL/min.

<sup>b</sup> $N = 5.54 \times (t_R / W_{0.5h})^2$ .

<sup>c</sup> $R_s = 1.18 \times |t_{R,n\text{-PEG}} - t_R| / (W_{0.5h,n\text{-PEG}} + W_{0.5h})$ , where  $t_R$  and  $t_{R,n\text{-PEG}}$  are the retention times, and  $W_{0.5h}$  and  $W_{0.5h,n\text{-PEG}}$  are the full width at half maximum of retention peaks of the PEG of interest and the referential *n*-PEG, respectively.

## 7. Supporting Figures

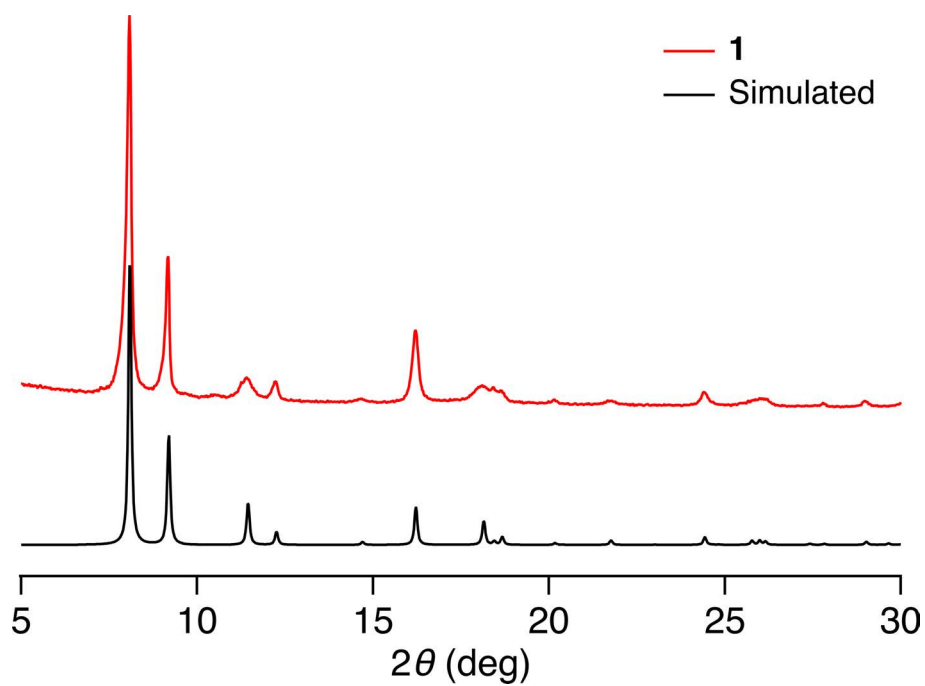


**Fig. S1.** PXRD data of **1**. The black line represents the simulated PXRD pattern of **1**.<sup>S1</sup> The observed PXRD pattern was in good agreement with the simulated one, confirming the successful synthesis of **1** particles.

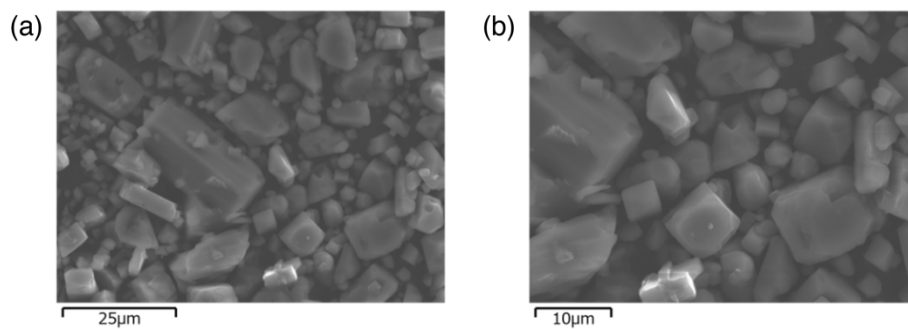


**Fig. S2.** SEM micrographs of **1** particles used for the MOF column preparation under (a)  $\times 1.5k$  and (b)  $\times 2.5k$  magnification. The particle size ranges approximately from 3 to 10  $\mu m$ .

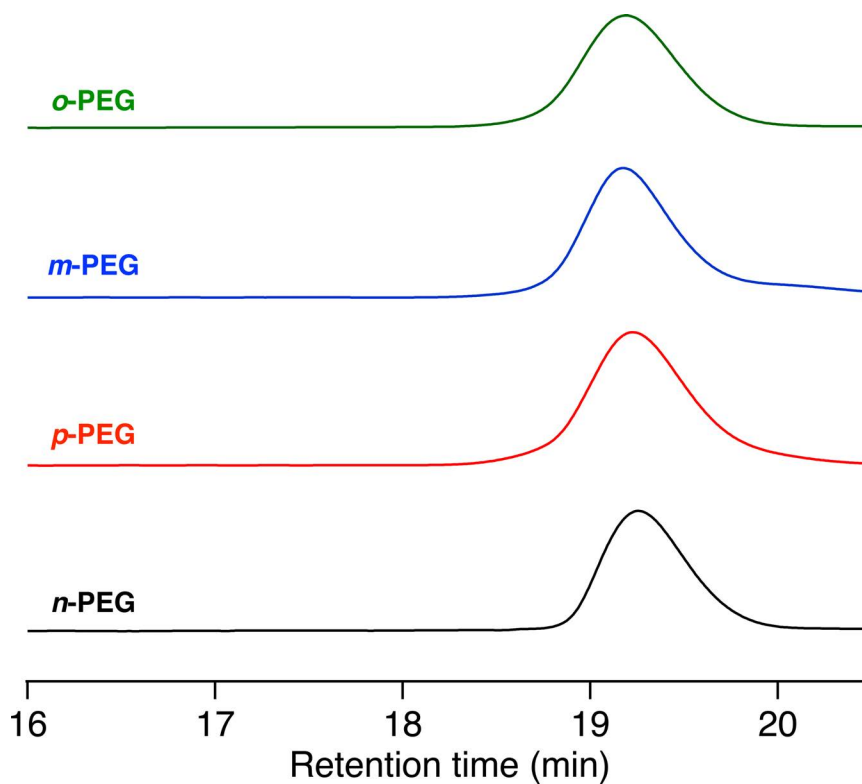


**Fig. S3.** SEC chromatograms of the model PEG samples. (green) *o*-PEG, (blue) *m*-PEG, (red) *p*-PEG, and (black) *n*-PEG. The molecular weights calculated based on the SEC data were summarized in Table S1. Since all the PEGs were prepared from the same PEG precursor (**PEG1k**) and dibromoxylene, their molecular weights should be identical.



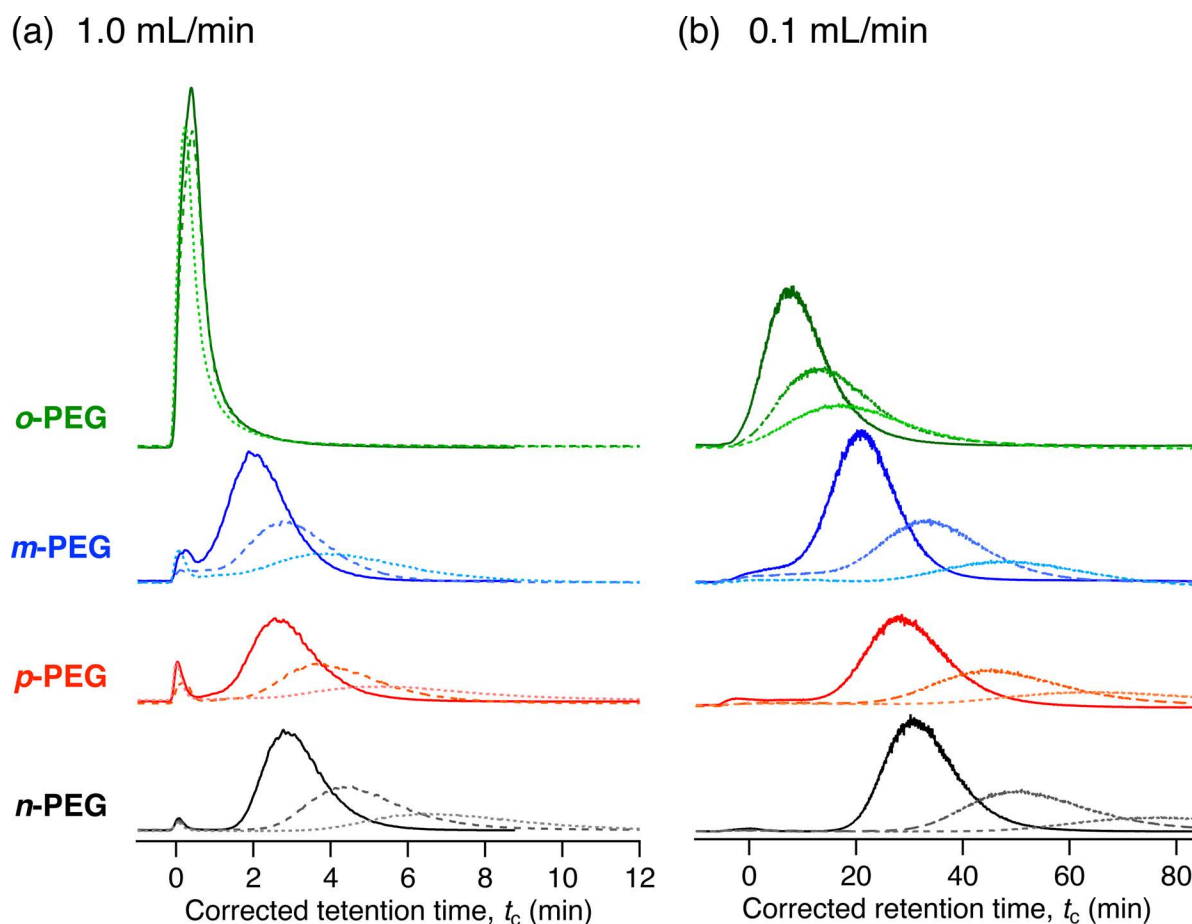


**Fig. S4.** Representative HPLC data of (green) *o*-PEG, (blue) *m*-PEG, (red) *p*-PEG, and (black) *n*-PEG measured at the flow rate of (a) 1.0 mL min<sup>-1</sup> and (b) 0.1 mL min<sup>-1</sup> on the **1**-packed column at (solid line) 80 °C, (dashed line) 70 °C, and (dotted line) 60 °C. A small front peak near  $t_0$  observed at 1.0 mL min<sup>-1</sup> is considered to be a so-called breakthrough peak.<sup>S8,S9</sup> Although the mechanism behind the breakthrough phenomenon in MOF-based LC is not yet fully understood, we believe that the significantly slow adsorption into MOF pores may be one of the causes of the breakthrough peaks observed with the PEGs. This assumption is supported by the fact that the breakthrough peaks diminish at lower flow rates (0.1 mL min<sup>-1</sup>).

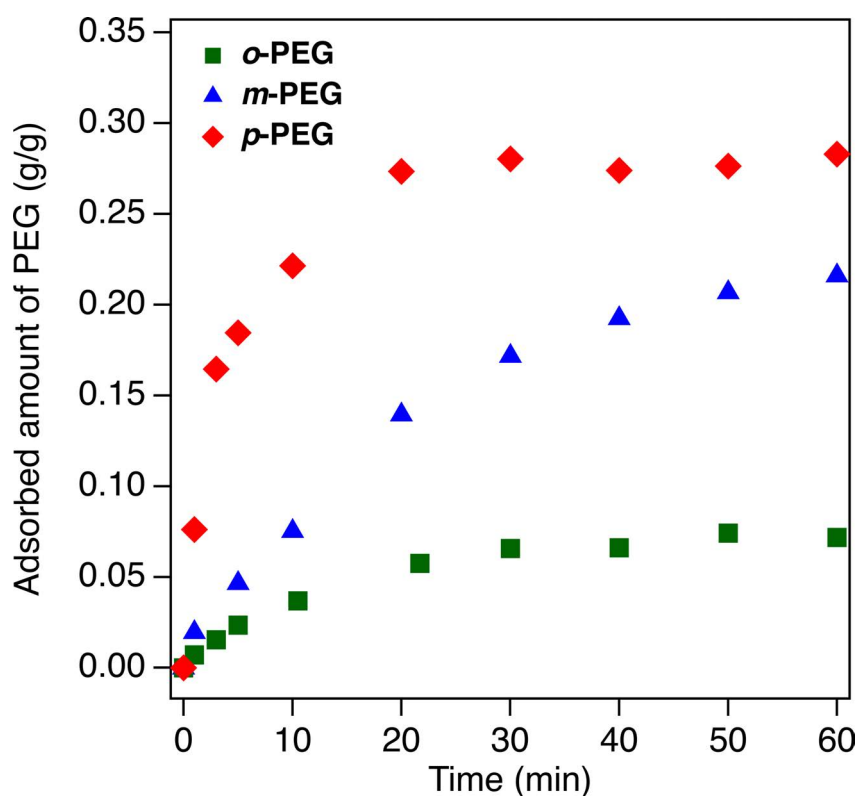


**Fig. S5.** Adsorption kinetics of (green squares) *o*-PEG, (blue triangles) *m*-PEG, and (red diamonds) *p*-PEG into **1**, measured in ethanol at 40 °C. The initial PEG concentration was 1.2 mg/g for all samples. *p*-PEG exhibited the fastest adsorption, while *o*-PEG had the slowest, with *m*-PEG showing an intermediate rate. These results suggest that adsorption in the narrow pores of **1** is influenced by the structure of the central xylene unit of the PEG chains.

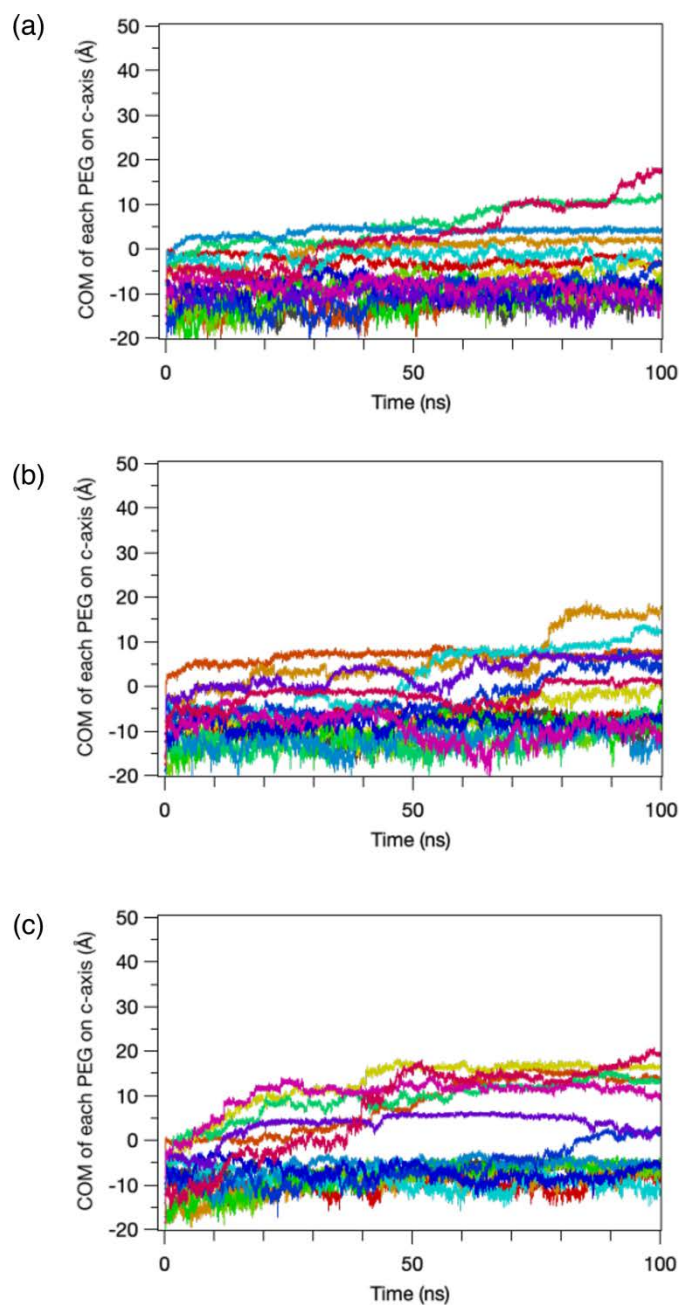


**Fig. S6.** Representative COM data of all 15 molecules of (a) *o*-PEG (20 mer), (b) *m*-PEG (20 mer), and (c) *p*-PEG (20 mer) infiltrating **1**, recorded in the typical MD run at 393 K for 100 ns. Each plot is color-coded by molecule. The origin ( $c = 0 \text{ \AA}$ ) is defined as the COM of Zn dimers of the paddle wheel cluster at the PEG/**1** interface. The infiltration occurs from the PEG molecules closest to the **1** surface. For *p*-PEG, diffusion into the pores is rapid, allowing the PEG chains to quickly penetrate deep into the MOF, while most of the *o*-PEG remains near the surface.

## 8. Supporting References

- (S1) H. Chun, D. N. Dybtsev, H. Kim and K. Kim, *Chem. Eur. J.*, 2005, **11**, 3521–3529.
- (S2) N. Mizutani, N. Hosono, B. Le Ouay, T. Kitao, R. Matsuura, T. Kubo and T. Uemura, *J. Am. Chem. Soc.*, 2020, **142**, 3701–3705.
- (S3) K. Kioka, N. Mizutani, N. Hosono and T. Uemura, *ACS Nano*, 2022, **16**, 6771–6780.
- (S4) N. Oe, N. Hosono and T. Uemura, *Chem. Sci.*, 2021, **12**, 12576–12586.
- (S5) A. P. Thompson, H. M. Aktulga, R. Berger, D. S. Bolintineanu, W. M. Brown, P. S. Crozier, P. J. in 't Veld, A. Kohlmeyer, S. G. Moore, T. D. Nguyen, R. Shan, M. J. Stevens, J. Tranchida, C. Trott and S. J. Plimpton, *Comput. Phys. Commun.*, 2022, **271**, 108171.
- (S6) A. Stukowski, *Model. Simul. Mater. Sci. Eng.*, 2010, **18**, 015012.
- (S7) B. Le Ouay, C. Watanabe, S. Mochizuki, M. Takayanagi, M. Nagaoka, T. Kitao and T. Uemura, *Nat. Commun.*, 2018, **9**, 3635.
- (S8) S. CHAPEL, F. Rouvière, V. Peppermans, G. Desmet and S. Heinisch, *J. Chromatogr. A*, 2021, **1653**, 462399.
- (S9) X. Jiang, A. van der Horst and P. J. Schoenmakers, *J. Chromatogr. A*, 2002, **982**, 55–68.